Available online at www.sciencedirect.com
SCIENCE DIRECT
Carbohydrate Polymers 62 (2005) 170–181
Carbohydrate Polymers
www.elsevier.com/locate/carbpol

Gelatinisation related structural aspects of small and large wheat starch granules

Rudi Vermeylen[a,*], Bart Goderis[b], Harry Reynaers[b], Jan A. Delcour[a]

[a]*Laboratory of Food Chemistry, Katholieke Universiteit Leuven, Kasteelpark Arenberg 22, B-3001 Heverlee, Belgium*
[b]*Laboratory of Macromolecular Structural Chemistry, Katholieke Universiteit Leuven, Celestijnenlaan 200F, B-3001 Heverlee, Belgium*

Received 2 May 2005; revised 21 July 2005; accepted 25 July 2005
Available online 8 September 2005

Abstract

Wheat starches from four European varieties (Charger, Estica, Skirlou and Soissons), and their small and large granule fractions were characterised on a structural level. Gelatinisation properties of starches and fractions thereof were compared. Isoamylase debranching revealed only limited differences between amylopectin chain lengths of the various starches and their fractions. Wide-angle X-ray diffraction, which showed predominant A-type crystallinity for all starches, revealed that large granules had systematically higher B-type and total crystallinity than small granules. Small-angle X-ray scattering (SAXS) indicated structural differences between amylopectins of distinct granule classes. At 42% moisture, the SAXS patterns of small granules were more intense than those of large granules, which, along with their higher gelatinisation peak temperature, suggested denser crystalline lamellae. Upon hydration from 42 to 66% moisture, small granules showed decreased lamellar repeat distances. As small granules displayed narrower helix–coil transition endotherms than large granules, shorter single stranded chains are envisaged to connect longer double helices to the amylopectin backbone in small wheat granules.

Keywords: Wheat starch; Small granules; Large granules; SAXS

1. Introduction

Starch, the main storage polysaccharide of plants, consists of amylopectin and amylose, both homo-polymers, with predominantly α-(1–4) linked glucose units, differing in molecular weight (MW) and degree of α-(1–6) branching. Amylopectin is of very high MW (ca. 10^8) and its cluster-like structure implies heavy branching (Hoseney, 1994). Amylose is the lower MW polymer (ca. 2.5×10^5), which behaves essentially as a non-branched entity (Hoseney, 1994). The double helices formed by the intertwining of amylopectin outer chains are arranged into crystalline register and impart semi-crystalline properties to starch. Starch itself is deposited into discrete granules in the amyloplasts of plant storage organs. In the endosperm of *Triticeae* (wheat, barley, rye, triticale) a bimodal starch granule size distribution, with large lenticular and small spherical granules is present (Shannon & Garwood, 1984). For wheat, deposition of large granules is initiated at approximately 4–12 days post-anthesis (Baruch, Meredith, Jenkins, & Simmons, 1979), and granules can grow throughout grain filling. Deposition of small granules is initiated between 16 and 22 days post-anthesis (Baruch et al., 1979) in protrusions stemming from amyloplasts containing lenticular granules (Langeveld, van Wijk, Stuurman, Kijne, & de Pater, 2000).

There are compositional differences between small and large wheat starch granules; small granules contain more lipids than large granules (Soulaka & Morrison, 1985a; Raeker, Gaines, Finney, & Donelson, 1998), while they generally have lower amylose contents (Soulaka et al., 1985a; Peng, Gao, Abdel-Aal, Hucl, & Chibbar, 1999). Furthermore, large barley (Tang, Ando, Watanabe, Takeda, & Mitsunaga, 2001) and wheat (Sahlström, Bævre, & Bråthen, 2003) starch granules show a larger proportion of long amylopectin chains (degree of polymerisation [DP]

Abbreviations: DP, degree of polymerisation; DSC, differential scanning calorimetry; HPAEC, high performance anion-exchange chromatography; MW, molecular weight; PAD, pulsed amperometric detection; SAXS, small-angle X-ray scattering; SCLCP, side-chain liquid crystalline polymer; WAXD, wide-angle X-ray diffraction.

* Corresponding author. Tel.: +32 1632 1634; fax: +32 1632 1997.
E-mail address: rudi.vermeylen@scarlet.be (R. Vermeylen).

0144-8617/$ - see front matter © 2005 Elsevier Ltd. All rights reserved.
doi:10.1016/j.carbpol.2005.07.021

24–30) than their small counterparts. On a higher structural level, large granules of barley (Tang et al., 2001) and wheat (Ando, Tang, Watanabe, & Mitsunaga, 2002) starches are more crystalline. Starch crystallites are accepted to be organised in lamellar structures (Cameron & Donald, 1992; Oostergetel & van Bruggen, 1989), but, to the best of our knowledge, no comparative information is available on the lamellar organisation in lenticular and spherical granules of *Triticeae*.

Small and large granules of barley and wheat starches show different behaviour in brewing (MacGregor & Morgan, 1986) and bread making (Sahlström et al., 2003; Soulaka & Morrison, 1985b), respectively. Divergence in functional properties can reasonably be expected to be provoked by differences in gelatinisation characteristics of both granule size-classes (Peng et al., 1999; Sahlström et al., 2003; Soulaka et al., 1985a).

In this study on a small set of European wheat starches and their small and large granule fractions, we corroborate previous results on amylopectin structure and crystallinity and gather new information on the lamellar organisation of these starches. We additionally relate data on the different levels of organisation to the gelatinisation characteristics of small and large granules in limited and excess water conditions.

2. Materials and methods

2.1. Parent starch

With a method described by Morrison, Milligan, and Azudin (1984), starches of four European winter wheats, grown in Belgium (Charger, Estica, Skirlou, and Soissons) were isolated. Yields ranged from 55 to 59 g starch (dm) per 100 g grain (dm).

2.2. Chemical analyses

Starch nitrogen content and damage were determined in duplicate according to Vandeputte, Vermeylen, Geeroms, and Delcour (2003). Apparent amylose content was determined colourimetrically according to Chrastil (1987). For determination of soluble amylose, dilute starch suspensions (1%, w/v) were heated at 95 °C for 30 min, and subsequently centrifuged (10 min, 1000 *g*). Soluble amylose was then measured in the resulting supernatants according to Chrastil (1987). Analyses were performed in triplicate. Standard errors were smaller than 5%.

2.3. β-amylolysis limit

Starch (6 mg) was solubilised by heating for 1 h at 100 °C in 0.5 ml sodium acetate buffer (pH 6.0, 0.02 N). β-limit dextrins were subsequently prepared according to Klucinec and Thompson (2002) and β-amylolysis limit was calculated from total carbohydrate (Dubois, Gilles, Hamilton, Rebers, & Smith, 1956) and reducing sugar (Somogyi, 1960) content of the solutions. Analyses were performed in triplicate. Standard errors were smaller than 5%.

2.4. Granule size distribution

Granule size distributions of parent starches were analysed using a Coulter Multisizer II (Coulter Electronics, Luton, UK) equipped with a 140 μm aperture tube and measuring in 256 channels, giving a measurements range between 2.8 and 84 μm. The equipment was calibrated with polystyrene–divinylbenzene latex. Starch samples were dispersed in sodium chloride solutions (5.0 g/L).

2.5. Starch fractionation

Aqueous suspensions (30%, w/v) of parent starches were fractionated into large and small granules by centrifugation (1000 *g*, 10 min) and subsequent pellet separation into top (enriched in small granules) and bottom (enriched in large granules) layers. This procedure was repeated three times on each of the top and bottom layers obtained. Finally, per variety, ultimate large and small granule fractions, respectively, accounting for 11.5–13.9% (w/w) and 8.2–9.9% (w/w) of the parent starches, were recovered.

2.6. Branch chain length distribution

Starch was debranched with isoamylase and its chain length distribution was determined with High Performance Anion-Exchange Chromatography (HPAEC) and Pulsed Amperometric Detection (PAD). Analyses were performed in duplicate according to Vermeylen, Goderis, Reynaers, and Delcour (2004). Individual peak areas in the chromatogram were corrected for molar PAD detector responses (Koch, Andersson, & Aman, 1998).

2.7. Crystallinity

Starches were equilibrated above a saturated sodium chloride solution at 23 °C, and powder wide-angle X-ray diffraction (WAXD) patterns were measured as described earlier (Vandeputte et al., 2003). Data were normalised to equal total scattering in the 6.5–33.0° 2θ range (with 2θ the diffraction angle obtained with Cu K_α-radiation of wavelength $\lambda = 1.54$ Å). Relative crystallinity was calculated based on comparison with reference patterns corresponding to the amorphous and various crystalline states (A, B-type) (Vermeylen et al., 2004). The level of amorphous, A-type and B-type material was estimated by minimising the sum of square error between the recording of the starch sample and the respective reference patterns.

2.8. Lamellar organisation

Small-angle X-ray scattering (SAXS) experiments with a slit-collimated primary beam were conducted on a Kratky camera, using Ni-filtered Cu K_α-irradiation generated by a Rigaku rotating anode device (Tokyo, Japan) operating at 40 kV and 60 mA. Scattering in the range $0.02 < s < 0.70\ nm^{-1}$ (with $s = 2\sin(\theta)/\lambda$ the modulus of the scattering vector) was detected with a one-dimensional Braun position-sensitive proportional detector, calibrated with silver behenate (Huang, Toraya, Blanton, & Wu, 1993). Samples were prepared as described earlier (Vermeylen et al., 2004), with a final moisture content of 41–43% for all starches. Parasitic scattering was subsequently removed by subtracting the scattering of an empty sample holder.

Pinhole SAXS patterns were collected at the DUBBLE CRG (Dutch-Belgian beamline) at the ESRF (Grenoble, France). An X-ray wavelength of 0.68 Å was used. The scattering angles at the 2D multiwire gas-filled SAXS detector, positioned at 2.5 m from the sample, were calibrated with silver behenate (Huang et al., 1993). Starch suspensions (66% water) were placed between two mica windows separated by a 2.0 mm brass spacer and equilibrated at 23 °C prior to data acquisition. The powder patterns were corrected for the detector response, and the intensity of the primary beam, measured by an ionisation chamber placed upstream from the sample, was used to calculate the sample transmission. The latter values served to properly subtract the pattern of an empty sample holder prior to averaging the 2D patterns azimuthally.

To allow for further data treatment, a constant background scattering caused by small-scale density fluctuations was estimated by fitting the appropriate Porod functions (Vonk, 1982) to the high angle tail (0.20–0.47 nm^{-1}) of the SAXS patterns. Background correction rendered $I_{exp}(s)$ and $\tilde{I}_{exp}(s)$ for samples recorded with point and slit geometry, respectively.

The random orientation of the crystalline and amorphous lamellae with respect to the X-ray beam was accounted for by the Lorentz correction, which was applied directly for the scattering patterns obtained with a point-collimated primary beam ($4\pi s^2 I_{exp}(s)$). $\tilde{I}_{exp}(s)$, resulting from starch interacting with the slit-collimated primary beam, was first desmeared to point collimation ($I(s)$) using the computer program TOPAS (Stribeck, 1993), and subsequently Lorentz corrected ($4\pi s^2 I(s)$). Bragg lamellar repeat distance (D_B) was calculated as $D_B = 1/s_p$, with s_p the scattering angle at peak intensity after Lorentz correction.

$I_{exp}(s)$ and $\tilde{I}_{exp}(s)$ were converted to real space by Fourier and Fourier–Bessel transformations, respectively (Vonk, 1982). The lamellar repeat distance (LP) was evaluated directly from the resulting linear correlation function, while the volume fraction of the crystalline lamellae in the lamellar stacks (φ) was obtained according to Goderis, Reynaers, Koch, and Mathot (1999).

The invariant of starch pellets (42% moisture) was approximated by integration of the smeared intensities in the range s 0.03–0.20 nm^{-1}: $Q_{ap} = \int \tilde{I}(s) s\, ds$, with Q_{ap}, the 'approximate' invariant. Theoretically, the observed invariant (Q) of systems with two small-scaled phases (e.g. stacked crystalline and amorphous lamellae) embedded in a third phase of much larger dimensions can be calculated by Eq. (1) (Goderis et al., 1999):

$$Q = \alpha(\Delta\rho_l)^2[\varphi(1-\varphi)] \quad (1)$$

Here, α represents the volume fraction of stacked lamellae, $\Delta\rho_l$ the electron-density difference between the amorphous and crystalline lamellae in the stack, and φ, as indicated above, the fractional lamellar crystallinity.

2.9. Gelatinisation characteristics

Differential scanning calorimetry (DSC) was carried out with a Seiko DSC-120 (Kawasaki Kanagawa, Japan). Approximately 6 mg starch was accurately weighed into aluminium sample pans, and water was added directly to obtain final moisture contents of 40 and 66%. Sample pans were hermetically sealed and equilibrated overnight. Samples at 40% moisture were heated from 25 to 155 °C at 4°/min, with an empty pan as reference. Calibration was with indium and tin. The transition temperatures (°C) reported are for onset (T_o), peak (T_p), and completion (T_c) of the G-endotherm (Donovan & Mapes, 1980), for the end of the M_1-endotherm (T_{end}), and for the peak of the M_2-endotherm (T_{aml}). Enthalpies (J/g dm) ΔH and ΔH_{aml} were determined by Seiko software by integrating the G- and M_2-endotherms, respectively. Analyses at 40% moisture were performed in triplicate. Starch samples suspended in excess water (66%) were heated from 25 to 95 °C at 4 °C/min. The heat capacity of the samples was balanced by adding water to the reference pan. The calibration was checked with benzophenone and α-naphtol standards. Transition temperatures (T_o, T_p, T_c) and enthalpy ΔH of the G-endotherm were determined in quadruplicate.

DSC-data of starches of different size classes (non-fractionated, small, large) of a single variety were compared and significance ($P = 0.05$) of differences was evaluated by the Tukey test for pairwise comparison. Two-factor analysis of variance was performed to evaluate influence of variety (factor levels: Charger, Estica, Skirlou, Soissons) and granule class (factor levels: small, large) on DSC parameters.

3. Results and discussion

3.1. Non-fractionated starches

In a first instance, non-fractionated starches were characterised. Low nitrogen (0.03–0.05%) and starch damage (0.8–1.0%) contents indicated purity and intactness.

Table 1
High performance anion exchange chromatography (HPAEC) based grouping of different DP fractions of debranched starch, wide-angle X-ray diffraction (WAXD) and small-angle X-ray scattering (SAXS) of wheat starches and their small and large granule fractions

Analysis	Debranching-HPAEC			WAXD		SAXS				
Starch source	DP[a] < 8 (mol%)	DP[a] 8–24 (mol%)	DP[a] > 24 (mol %)	Crystallinity		D_B (42%)[b] (nm)	LP (42%)[c] (nm)	D_B (66%)[b] (nm)	LP (66%)[c] (nm)	Q_{ap} (42%)[d] (a.u.)
				Total (%)	B-type (%)					
Charger										
Total	2.7	83.2	14.1	35	3	9.5	8.8	9.5	8.9	2.1
Small	3.0	83.4	13.6	32	0	9.7	8.7	9.3	8.7	2.5
Large	3.4	82.4	14.2	37	3	9.5	8.8	9.6	9.0	2.0
Estica										
Total	3.0	82.3	14.8	33	4	9.4	8.7	9.5	9.0	2.1
Small	3.1	82.8	14.1	31	1	9.6	8.8	9.3	8.9	2.3
Large	3.5	81.8	14.8	35	6	9.4	8.7	9.6	9.0	1.9
Skirlou										
Total	3.4	82.0	14.6	33	0	9.7	9.0	9.6	9.1	2.1
Small	3.5	81.7	14.9	30	0	9.8	8.9	9.5	9.0	2.5
Large	4.0	81.1	14.9	37	2	9.7	9.0	9.7	9.2	1.9
Soissons										
Total	3.2	82.2	14.6	36	4	9.3	8.7	9.4	8.8	2.0
Small	2.9	83.0	14.1	34	0	9.5	8.6	9.1	8.5	2.5
Large	3.8	81.6	14.6	37	5	9.2	8.7	9.5	8.9	1.9
Repeatability[e]	0.3	0.4	0.3	2	1	<0.1	0.1	<0.1	0.1	0.1

[a] Degree of polymerisation.
[b] Bragg spacing for starches at 42 and 66% moisture, respectively.
[c] Lamellar repeat distance from correlation function analysis for starches at 42 and 66% moisture, respectively.
[d] Approximate invariant for starches at 42% moisture.
[e] Standard deviation from fourfold analysis of a single starch sample.

All starches had similar apparent amylose contents (37.0–37.9%). Compared to most reported values (Buléon, Colonna, Planchot, & Ball, 1998), the apparent amylose contents were high and coincided with the upper limit of colourimetrically determined amylose contents found in a set of 200 hexaploid wheats (36%; Stoddard & Sarker, 2000). Total amylose content largely exceeded the level of amylose solubilised under the experimental conditions (20.3–23.8%). Similar observations were made earlier for rice starches (Reddy, Ali, & Bhattacharya, 1993), where the difference between soluble and total apparent amylose correlated with the level of extra long amylopectin chains. Such chains also occur in wheat starches (Hizukuri, 1996), but assignment of the 'insoluble amylose' fraction observed in the present study to extra long amylopectin chains is speculative. β-amylolysis results failed to reveal differences between starches (55.7–57.1%). The HPAEC-chromatograms of isoamylase debranched starches were essentially similar as well (Table 1).

Limited differences in the crystallinities of the parent starches were observed (Table 1). Soissons (crystallinity: 36%) and Charger starches (35%) were slightly more crystalline than Skirlou and Estica starches (both 33%). Diffractograms (Fig. 1) showed predominant A-type crystallinity, but the intensity of the 5.5° 2θ peak, which is typical for B-type crystalline unit cell, differed among samples and was most prominent for Estica and Soissons.

SAXS measurements on both moist pellets (41–43% moisture) and suspensions (66% water) of parent starches revealed only small differences in the Bragg lamellar repeat distance (D_B) and the lamellar repeat distance obtained from correlation analysis (LP) (Table 1). Moreover, total scattered intensity at 42% moisture, as indicated by the approximate invariant, was similar for all parent starches (Table 1). As semi-crystalline growth rings in starch

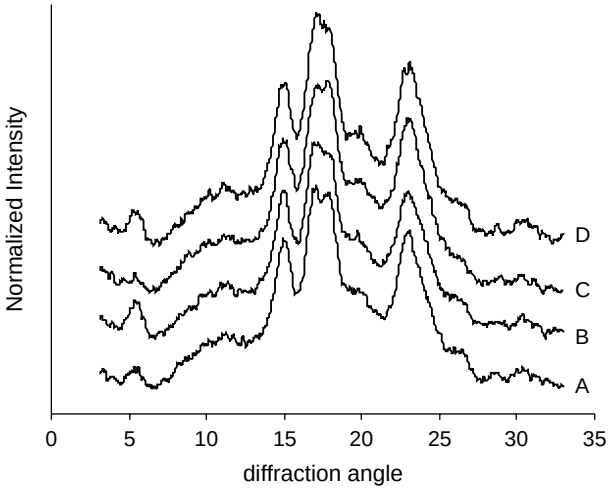

Fig. 1. Wide-angle X-ray diffraction patterns of wheat starches (normalised and shifted along the ordinate for clarity), Charger (A), Estica (B), Skirlou (C), Soissons (D).

granules have dimensions (120–400 nm; French, 1984) largely exceeding the lamellar repeat distance (9–11 nm), the small-angle scattering in the experimentally assessed window is dominated by the alternating amorphous and crystalline lamellae. Consequently, results indicate similarity in the average structure of the alternating crystalline and amorphous lamellae in the semi-crystalline growth-rings of the starches.

Although starch yields were similar for the four varieties (55–59 g/100 g grain), granule-size distributions showed large differences (Fig. 2). Small spherical granules displayed modal dimensions of 5–7 μm, while large lenticular granules with modal dimensions of 15–19 μm had a diameter up to 40 μm, in accordance with literature (Soulaka et al., 1985a; Vansteelandt & Delcour, 1999). Although environment and temperature influence the size and the level of granules in each size class (Shi, Seib, & Bernardin, 1994; Soulaka et al., 1985a), the large heterogeneity observed in the present study most probably reflects varietal differences, which have major effects on granule-size distribution (Dengate & Meredith, 1984; Raeker et al., 1998).

Fig. 3 shows DSC thermograms, with indications of some relevant transition temperatures. At 40% moisture a small G-endotherm (2.7–2.9 J/g), ascribed to starch gelatinisation (Donovan et al., 1980), was followed by a broad M_1-endotherm similar for all starches. The latter endotherm has been attributed to either a melting of incompletely solvated starch crystallites (Donovan et al., 1980) or, more recently, to the helix–coil transition of amylopectin double helices (Waigh, Gidley, Komanshek, & Donald, 2000). The M_2-endotherm at 120 °C is caused by dissociation of amylose–lipid complexes (Donovan et al., 1980). In excess water, disruption of amylopectin resulted in a single endotherm (50–65 °C, 13.3–14.0 J/g), which was asymmetric for Estica and Skirlou starches. These starches displayed a weak high-temperature shoulder (65–74 °C), which did not disappear when the moisture content was

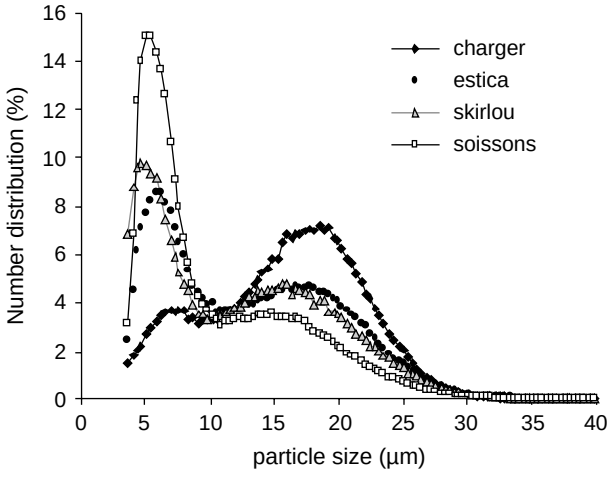

Fig. 2. Granule size number distribution of wheat starches.

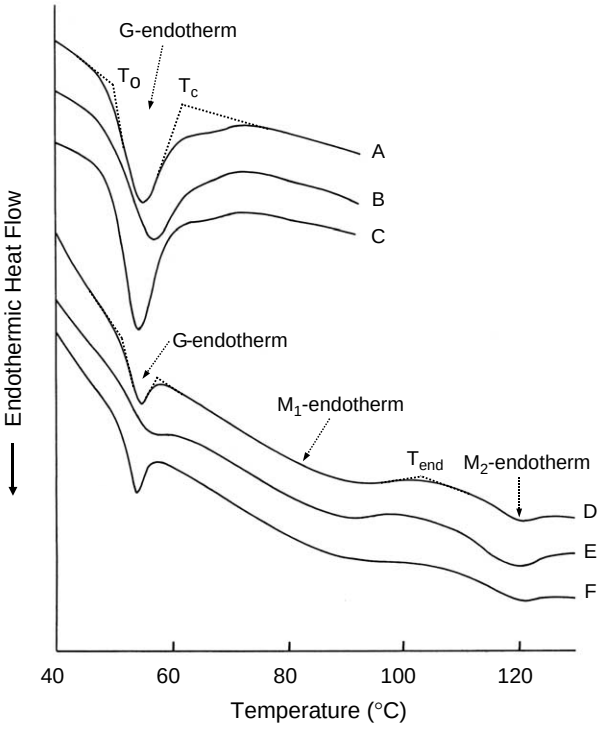

Fig. 3. Differential scanning calorimetry of non-fractionated Estica starch (A, D) and its small (B, E) and large (C, F) granule fractions at 66% (A, B, C) and 40% (D, E, F) moisture. Onset and conclusion of the G-endotherm, and end of M_1-endotherm are indicated by T_o, T_c, and T_{end}, respectively. Thermograms are shifted along the ordinate for clarity.

increased further (results not shown). In literature, high gelatinisation enthalpies have been related to high crystallinities (Qi et al., 2004; Vandeputte et al., 2003). A similar trend, although not well pronounced, was observed here. Onset (51.2–55.2 °C at 40%, and 49.0–54.0 °C at 66% moisture) and peak (54.6–58.3 °C at 40% moisture) temperatures of gelatinisation varied considerably among parent starches, but no obvious relations with structural characteristics were observed. Furthermore, Estica and Soissons starches showed larger gelatinisation ranges. Work described below indicates that this does not relate to a larger structural heterogeneity as might be suggested by a larger portion of B-type crystals.

3.2. Large and small granule fractions

A more detailed examination of structure–gelatinisation relations was undertaken by analysing separately large and small granules. The total content of large, lenticular granules in wheat starch ranges from 65 to 87% by weight (Soulaka et al., 1985a). In this study, however, a complete fractionation of the parent starch was not aimed for. Instead the most extreme large and small granule fractions, accounting on average for 12 and 9% of the starch weight, were retained. Effectiveness of the separation procedure was judged from light-microspcopy (results not shown).

HPAEC revealed small but consistent differences between amylopectin chains obtained from isoamylase debranched small and large granules (Table 1). Short and intermediate-length chains with DP 8–24 were more abundant in the small granule fractions, while very short (DP < 8) and long (DP 25–60) chains were somewhat more numerous in large granules. The latter observation concurs with previous reports (Sahlström et al., 2003; Tang et al., 2001). In contrast, Sahlström et al. (2003) found that small granules contain a larger proportion of the shortest amylopectin chains (DP < 8).

Small granules were generally less crystalline than their large counterparts (Table 1). The difference was most marked for Skirlou starch. As such, these results corroborate recent work of Ando et al. (2002). The positions of the characteristic A-type diffraction peaks are independent of granule size, indicating equal density within individual starch crystallites in the different starch fractions. The wheat starches examined furthermore showed secondary B-type crystallinity (cf. supra), which was absent in the small granule fractions (Fig. 4).

Small granules had systematically larger Bragg lamellar repeat distances at 42% moisture than large granules (Table 1). It is of note that Bragg spacings accurately describe the average repeat distance only when no long-range disorder is present (i.e. when dimensions of all lamellae within semi-crystalline growth rings are identical). The larger the long-range disorder, the more Bragg spacings will overestimate the effective number average repeat distance (Crist, 2000). A better estimate for the number average repeat distance is obtained from correlation function analysis. The LP thus obtained is similar for all granule fractions (Table 1). This indicates that a larger long-range disorder rather than an effective difference in the number average lamellar repeat distance is responsible for the larger Bragg distance of the small granules at 42% moisture.

At higher moisture contents (66%), the difference between D_B and LP becomes markedly smaller for the small granule fractions. In line with the above, this might indicate an increased long-range order within the semi-crystalline growth rings. According to Waigh, Perry, Riekel, Gidley, and Donald (1998), lamellar periodicity develops on hydration of dry starch from 5 to 40% moisture. It is not unreasonable that some further rearrangements can take place at higher moisture levels. Compared to the large granules, small granules had larger long-range disorder at 42% moisture (cf. supra), and the increased ordering of their lamellar structure at higher moisture levels should probably be regarded as a postponed ordering process. The latter could be similar to the nematic to smectic transition proposed by Donald and co-workers (Donald, 2001; Waigh et al., 1998) in their side-chain liquid-crystalline polymer (SCLCP) view on amylopectin. In line with this thinking, it is anticipated that higher moisture contents are needed to efficiently decouple the mesogens (double helices) from the mobile molecular backbone in small wheat granules. On a molecular level, flexible spacers (i.e. single stranded parts of amylopectin connecting double helices to the amylopectin backbone) are thus assumed to be shorter in the small granule fraction.

At 42% moisture, small granules clearly scattered more intensively than large granules (Fig. 5). Remarkable differences in scattering power have been observed earlier between amylose deficient and regular starches (Jenkins & Donald, 1995; Vermeylen et al., 2004; Yuryev et al., 2004). The more intense scattering in the former was, at least partially, explained by the more pronounced electron density difference between amorphous and crystalline

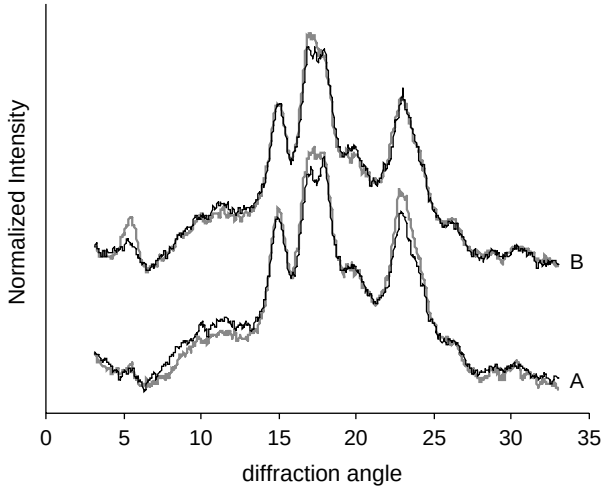

Fig. 4. Wide-angle X-ray diffraction patterns of small (thin black line) and large (bold gray line) wheat starch fractions of Estica (A) and Skirlou (B). Patterns were normalised and per variety shifted along the ordinate for clarity.

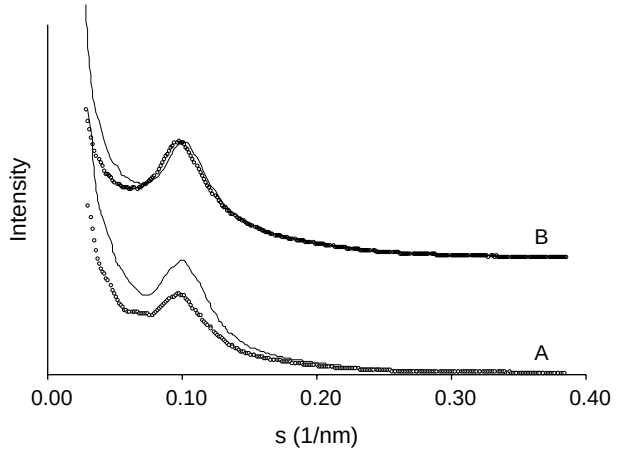

Fig. 5. Small-angle X-ray scattering patterns of small (full line) and large (dotted line) granule fractions of Estica starch: (A) desmeared scattering data on moist pellets (42% moisture), (B) pinhole measurements on suspensions (66% moisture) scaled to the same peak intensity and shifted along the ordinate for clarity.

lamellae. It is known from literature (Peng et al., 1999; Soulaka et al., 1985a) that small wheat starch granules have lower amylose contents than large ones. It might be tempting to conclude that, in large lenticular wheat granules, amylose prevents optimal packing of amylopectin double helices into crystalline lamellae, by either co-crystallisation with amylose (Jenkins et al., 1995), or amylose tie-chains (Yuryev et al., 2004). However, it is hard to grasp how amylose, which is predominantly present in the amorphous growth rings (Blennow, Hansen, Schultz, Jørgensen, Donald and Sanderson, 2003), would disturb crystalline lamellae in the semi-crystalline growth rings. In view of the SCLCP concept, the possibility that subtle differences in the amylopectin fine structure might affect the lamellar organisation of small and large granules should be considered, however. Therefore, a tentative structural model is proposed in Section 4.

In a recent paper on mutant wheat starches (Yuryev et al., 2004), differences in SAXS intensities were ascribed to larger density differences between amorphous and crystalline lamellae. An improved density contrast may indeed explain the higher SAXS intensity of small wheat granules. However, according to the definition of the invariant (Eq. (1)), also the volume fractions of (1) the crystalline growth rings (i.e. the lamellar stacks, α), and (2) the crystalline lamellae within the crystalline growth rings (φ) may influence small-angle scattering. The lower WAXD crystallinity observed for the small granule fractions seems not to be in line with the larger fraction of crystalline growth rings needed to account for its higher SAXS intensity. On the other hand, a positive relation between WAXD crystallinity and φ might rationalise the higher small-angle scattering intensity of the small granules. However, correlation function analysis rendered similar estimates for φ of all starch fractions (0.75–0.77), which indicates that fractional lamellar crystallinity is unlikely to cause the large variation in Q. Hence, the more intense scattering of the small granule fractions hydrated at 42% is most probably engendered by differences in $\Delta\rho_l$.

Measurements on starch suspensions (66% water) were not absolute in view of the insufficient control on the irradiated sample mass. As such, the higher scattered intensity of small granules at 42% moisture could not be confirmed experimentally for more hydrated starch fractions. However, as the shift in Bragg spacings upon hydration of small granules is presumably caused by the further development of the lamellar structure, $\Delta\rho_l$ is anticipated to increase further. X-ray analyses thus suggest a relatively denser packing of amylopectin double helices in the crystalline lamellae of small wheat starch granules.

Pinhole measurements (excess water) and desmeared scattering patterns (42% moisture) revealed higher intensities at $s < 0.07\ \mathrm{nm}^{-1}$ for the small granules, which were initiated later in starch development (Fig. 5). Similarly, analyses on growth series of waxy maize and normal maize starches displayed a systematic increase of the scattering in

Table 2
Differential scanning calorimetry onset (T_o), peak (T_p), and completion (T_c) temperatures and enthalpies (ΔH) of the G-endotherm, completion temperature (T_{end}) of M_1-endotherm and peak temperature (T_{aml}) and enthalpy (ΔH_{aml}) of the M_2-endotherm of wheat starches and their small and large granule fractions measured at 40% moisture

Starch source	G-endotherm					M_1-endotherm		M_2-endotherm	
	T_o (°C)	T_p (°C)	T_c (°C)	$T_c - T_o$ (°C)	ΔH (J/g)	T_{end} (°C)	$T_{end} - T_c$ (°C)	T_{aml} (°C)	ΔH_{aml} (J/g)
Charger									
Total	53.6^{A}	56.6^{B}	59.7^{B}	6.1^{B}	2.8^{A}	103.3^{BC}	43.5^{B}	119.9^{BC}	1.0^{B}
Small	52.6^{B}	57.1^{A}	61.9^{A}	9.3^{A}	2.8^{A}	98.9^{AB}	37.0^{A}	119.3^{AB}	1.9^{A}
Large	53.4^{A}	56.0^{C}	58.7^{C}	5.3^{C}	2.9^{A}	106.4^{C}	47.7^{B}	120.7^{C}	0.9^{B}
Estica									
Total	51.2^{A}	54.6^{B}	57.6^{B}	6.4^{B}	2.8^{A}	102.0^{BC}	44.4^{B}	120.5^{A}	1.0^{B}
Small	50.9^{A}	56.0^{A}	61.3^{A}	10.4^{A}	2.5^{A}	98.9^{AB}	37.6^{A}	119.6^{A}	1.9^{A}
Large	51.1^{A}	54.0^{C}	56.7^{C}	5.6^{B}	2.8^{A}	103.1^{C}	46.4^{B}	120.6^{A}	0.8^{B}
Skirlou									
Total	55.2^{A}	58.3^{A}	61.1^{B}	5.9^{B}	2.7^{A}	103.5^{B}	42.3^{AB}	119.8^{BC}	0.8^{B}
Small	52.7^{B}	57.5^{B}	63.0^{A}	10.3^{A}	2.5^{A}	100.7^{A}	37.7^{A}	119.4^{AB}	1.8^{A}
Large	54.9^{A}	57.4^{B}	59.9^{C}	5.0^{B}	2.8^{A}	104.3^{B}	44.4^{BC}	120.8^{C}	0.8^{B}
Soissons									
Total	52.0^{A}	56.3^{B}	59.9^{B}	8.0^{B}	2.9^{A}	104.4^{B}	44.5^{B}	120.7^{B}	0.8^{A}
Small	52.6^{A}	57.5^{A}	63.6^{A}	11.0^{A}	2.8^{A}	98.8^{A}	45.1^{A}	119.6^{A}	1.8^{A}
Large	52.5^{A}	55.5^{C}	58.4^{C}	5.9^{C}	2.8^{A}	106.9^{B}	48.5^{B}	121.0^{B}	0.7^{B}
Two factor ANOVA[a]									
Variety	NS	**	**	NS	NS	NS	NS	NS	NS
Particle class	NS	**	**	**	NS	*	**	*	**

Different characters indicate significant differences (among fractions of a single variety) on 5% level according to the Tukey test. Level of significance are indicated: $^{**}P < 0.0001$, $^{*}P < 0.05$, NS: non-significant ($P > 0.05$).

[a] Two factor analysis of variance (ANOVA) with Charger, Estica, Skirlou and Soissons the factor levels of 'variety', and Small and Large the factor levels of 'particle class'.

the ultra low angle region (Donald et al., 1997). It has been put forward that this results from a decreasing density of the amorphous growth rings during starch deposition.

At limited moisture (40%), small granules had either similar (Estica, Soissons) or lower (Charger, Skirlou) T_o than large granule fractions (Table 2). With the exception of Skirlou starch, small granules had higher T_p, while T_c was higher for the small granule fractions of all investigated wheat varieties. The small G-endotherm (2.5–2.9 J/g) was hence broader (T_c–T_o, Table 2) for the small granule fractions than for their large counterparts. Contiguous to the G-endotherm, DSC thermograms displayed broad M_1-endotherms, which ended at significantly lower temperatures (T_{end}) for the small wheat granules. Similar observations have been made for small and large granule barley starches (Myllärinen, Schulman, Salovaara, & Poutanen, 1998), but no explanation was given. The width of the M_1-endotherm was estimated by T_{end}–T_c (Table 2), as the conclusion of the G-endotherm (T_c) virtually coincided with the onset of the M_1-endotherm. As mentioned above, the M_1-endotherm under limited moisture conditions has been ascribed to the helix–coil transition, a cooperative process occurring over smaller temperature ranges when the (double) helix is longer (Waigh et al., 2000). Accordingly, small granules, which have a narrower helix dissociation endotherm (Table 2), would have longer double helices. Around 120 °C, the small granules displayed a much larger amylose–lipid dissociation endotherm than large granules (1.9 vs. 0.8 J/g), which reflects the higher lipid content of small wheat granules (Raeker et al., 1998; Soulaka et al., 1985a). In excess water, the G-endotherm is much larger (12.5–13.9 J/g), but the gelatinisation temperatures of the different particle classes related similarly as at 40% moisture. In accordance with literature (Peng et al., 1999; Sahlström et al., 2003; Soulaka et al., 1985a), small granule wheat starch fractions gelatinised at higher temperatures (T_p, T_c) and over a broader temperature range than their large granule counterparts (Table 3). With the exception of Skirlou starch, particle class did not influence T_o of individual varieties.

4. General discussion

Knowledge on the length of double helices, and their packing in crystallites (WAXD) and lamellae (SAXS) is combined in an integrated view on (1) macromolecular structural differences between small and large wheat granules, and (2) their gelatinisation characteristics.

4.1. Structural model

Despite the fact that large granules, in contrast to its small analogues, show marked B-type crystallinity, only limited differences between granule fractions were found for the amylopectin chain length distribution. In literature, B-type amylopectin crystallites have been suggested to differ from A-type crystallites in (1) chain length and (2) branching pattern. On the one hand, (1), B-type crystallinity is related to longer (average) amylopectin chains (Hizukuri,

Table 3
Differential scanning calorimetry onset (T_o), peak (T_p), and completion (T_c) temperatures, and enthalpies (ΔH) of the G-endotherm of wheat starches and their small and large granule fractions measured at 66% moisture

Starch source	T_o (°C)	T_p (°C)	T_c (°C)	T_c–T_o (°C)	ΔH (J/g)
Charger					
Total	52.0^{A}	56.7^{B}	62.1^{B}	10.1^{B}	13.7^{A}
Small	51.4^{A}	57.3^{A}	63.7^{A}	12.3^{A}	13.5^{A}
Large	51.8^{A}	56.1^{C}	60.8^{C}	9.0^{C}	13.9^{A}
Estica					
Total	49.0^{A}	55.2^{B}	62.4^{B}	13.4^{B}	13.3^{A}
Small	49.1^{A}	56.9^{A}	64.8^{A}	15.7^{A}	12.7^{A}
Large	49.3^{A}	54.4^{C}	60.4^{C}	11.1^{C}	13.8^{A}
Skirlou					
Total	54.0^{A}	58.3^{A}	63.2^{B}	9.1^{B}	13.3^{A}
Small	52.3^{B}	58.0^{AB}	64.1^{A}	11.8^{A}	12.5^{A}
Large	53.8^{A}	57.7^{B}	62.1^{C}	8.4^{C}	13.3^{A}
Soissons					
Total	51.5^{A}	57.2^{B}	63.3^{B}	11.7^{B}	14.0^{A}
Small	51.7^{A}	58.3^{A}	65.3^{A}	13.6^{A}	13.7^{A}
Large	51.3^{A}	56.1^{C}	61.3^{C}	10.0^{C}	13.7^{A}
Two factor ANOVA[a]					
Variety	**	**	NS	NS	NS
Particle class	NS	**	**	**	NS

Different characters indicate significant differences (among fractions of a single variety) on 5% level according to the Tukey test. Levels of significance are indicated: $^{**}P<0.0001$, $^{*}P<0.05$, NS: non-significant ($P>0.05$).

[a] Two factor analysis of variance (ANOVA) with Charger, Estica, Skirlou and Soissons the factor levels of 'variety', and Small and Large the factor levels of 'particle class'.

1986). However, as the occurrence of B-type crystallites in wheat starches is related to lower temperatures during grain-filling (Buléon et al., 1999), and as oligosaccharides tend to crystallize into the B-allomorph at shorter chain lengths under these temperature conditions (Hizukuri, Takeda, Usami, & Takase, 1980), a clear relation between amylopectin external chain length and B-type crystallinity might be clouded by temperature differences during the grain-filling period. On the other hand, (2), the amylopectin clusters of starches characterised by the less dense B-type crystalline unit cell were smaller and less densely branched than those of A-type starches (Gérard, Planchot, Colonna, & Bertoft, 2000; Hanashiro, Tagawa, Shibahara, Iwata, & Takeda, 2002). Similar relations between crystal type and amylopectin branching structure may hold for wheat starches. Several starch branching enzymes are indeed specifically associated with large wheat starch granules, and are absent in small granule fractions (Peng, Gao, Båga, Hucl, & Chibbar, 2000). These enzymes are perhaps the biochemical key to B-type crystallinity in large lenticular granules.

Fig. 6 illustrates how variation of the branching pattern, leaving the amylopectin chain length distribution unaltered, can result in (1) a different contrasts between amorphous and crystalline lamellae, and (2) an altered tendency toward B-type crystallinity. In passing from panels A to B (Fig. 6), only the position of the amylopectin branch points is changed. This results in longer flexible spacer and shorter double helix lengths in B. In this view, neither the orientation nor the lateral position of double helices in the crystalline lamellae are considered. By lateral movement of the double helices in panel B, situation C is obtained. Such a translation is anticipated from the positive relation between inter-double helix distance and chain length of the single-stranded chains interconnecting them (O'Sullivan & Pérez, 1999). On the other hand, an increase in flexible spacer length may allow double helices that were poorly decoupled from the molecular backbone (panel A) to become incorporated into crystallites, which themselves do not have to align perfectly in the crystalline lamella (panel D).

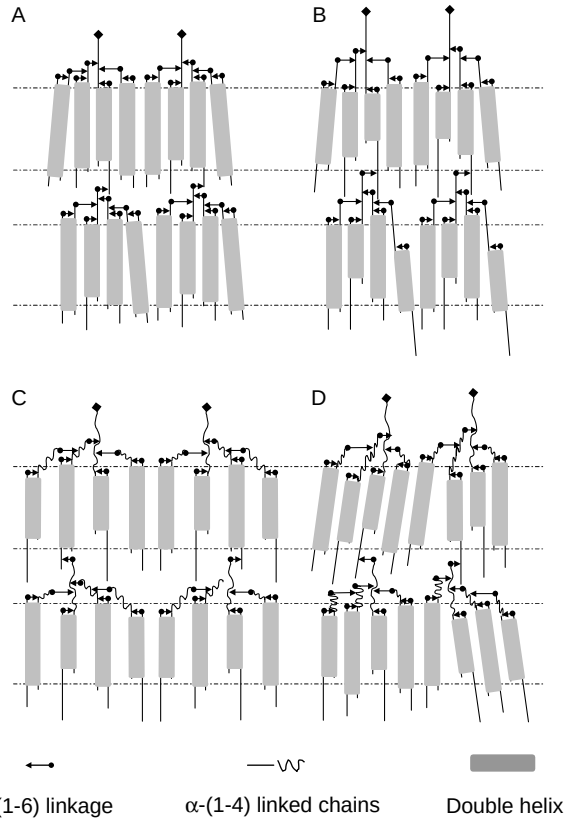

Fig. 6. Schematic representation of effects of altered branching patterns (A vs. B, C, D) on the lamellar structure of amylopectin. Detailed discussion is presented in the text.

In this study, amylopectin chain length distribution of small and large granule fractions differed only marginally, but DSC pointed out that double helices were longer in small wheat granules (cf. supra). The latter corresponds to panel A (Fig. 6). A reduction of the amylopectin outer branch-length (panel B) thwarts the optimal filling of the crystalline lamellae, and may account for the lower density of the crystalline lamellae in the large granules. Furthermore, the lateral movement of double helices (panel C, Fig. 6) decreases double helix density and may account for the larger tendency towards B-type crystallinity, as the corresponding crystalline unit cell has a lower density than A-type crystallites (Imberty, Buléon, Tran, & Pérez, 1991). The above might explain the higher level of B-type crystallites in large wheat starch granules. However, unlike the differences in B-type crystallinity, the difference between the 'approximate invariant' of large and small granule fractions is not sample dependent. The hypothetical structure in panel C (Fig. 6) can thus only partially account for the different scattering behaviour of both granule fractions. WAXD indicated furthermore that the density within individual A-type crystals was similar in large and small granules. Thus, not the packing of double helices in the crystallites, but the alignment of crystallite sub-units (clusters of double helices) into 'crystalline' lamellae may be primarily responsible for the differences in small-angle scattering power between large and small wheat starch granules. The mosaic appearance of the crystalline lamellae, as presented in panel D (Fig. 6), is in line with this line of thinking. Moreover, the packing of 'loose double helices' into crystalline register might explain the higher crystallinity of the large wheat starch granules.

To conclude, it is speculated that lamellar structures in small wheat granules resemble the structural model presented in panel A. A subtle alteration of amylopectin branching pattern, resulting in a combination of the structures shown in panels B, C and D, is proposed to be responsible for the modified WAXD and SAXS characteristics of large wheat granules.

4.2. Gelatinisation

In polymer science, melting of lamellar crystallites is often evaluated by the Gibbs–Thomson equation (Eq. (2)), with: T_m^0, ΔH^0 the melting temperature (K) and enthalpy (J g^{-1}) of the perfect infinitely sized crystallite, respectively; γ, ρ_c, and D_c, the interfacial tension (surface free energy in J m^{-2}), density (g m^{-3}) and thickness (m) of the non-perfect crystallite

$$T_m = T_m^0\left[1-\frac{2\gamma}{\Delta H^0 \rho_c D_c}\right] \quad (2)$$

Accordingly, higher gelatinisation temperatures of crystallites in small granules may be caused by (1) less defective crystallites with sharp interfaces (lowering γ; Bocharnikova et al., 2003; Wasserman, Eiges, Koltysheva, Andreev, Karpov and Yuryev, 2001), (2) a change of the crystal polymorphous structure (i.e. variation in type of crystalline unit cell) (affecting T_m^0 and ΔH^0; Whittam, Noel, & Ring, 1990), (3) larger crystallite dimensions (increasing D_c; Qi et al., 2004), and (4) a higher density of the crystalline lamella (increasing ρ_c). Relevance of these theoretical parameters to the dissimilar gelatinisation of small and large granules is discussed below.

(1) The accumulation of defects during starch biosynthesis (Protserov, Karpov, Kozhevnikov, Wasserman, & Yuryev, 2000; Wasserman et al., 2001) would cause large granules, which were deposited over a longer time period, to gelatinise, on average, at lower temperatures. The relatively large proportion of very short amylopectin chains (DP < 8) in the large granule fractions presumably act as crystal defects.
(2) Effects of variation in the crystalline unit cell are expected to be of minor importance in determining the gelatinisation temperatures of small and large wheat granules, as peak positions typical for the A-type unit cell are unaffected by particle class, and the presence of B-type crystallinity accounts for 0–17% of total starch crystallinity.
(3) The longer double helix length in small wheat granules, derived from DSC at lower moisture contents, seems to be in line with the thicker lamellar crystallites suggested by the Gibbs–Thomson equation. From SAXS analyses, indications of the average thickness of the crystalline lamellae (C) can be obtained through $C = \mathrm{LP}\varphi$. As φ is similar for both granule fractions and LP is slightly larger for the large granule fraction, SAXS does not point out thinner crystalline lamellae in large wheat granules.
(4) A higher density of the crystalline lamellae may account for both the higher gelatinisation temperature and the higher SAXS intensities observed for small wheat granules. Small granules had systematically larger fractions of A and B_1 amylopectin chains (DP 8–24; Table 1), which moreover were organised to give longer double helices, and hence more perfectly filled (and denser) crystalline lamellae.

As noticed above, the gelatinisation range is often interpreted in terms of heterogeneity of starch crystallites. The role of crystallinity here seems of only secondary importance, as starches with the most heterogeneous crystal structures (large granule fractions) displayed the smallest gelatinisation range (Table 2). However, gelatinisation is a granule per granule event, with individual starch granules gelatinising in a 1 °C temperature range in excess water (French, 1984). Accumulation of crystallite defects (cf. supra) would hence trigger the gelatinisation, measured on a bulk of granules, to occur over a smaller temperature range for the large granules because its number of granules per weight is lower (Vasanthan & Bhatty, 1996).

5. Conclusions

Wheat starches displayed predominant A-type crystallinity, with an appreciable level of B-type crystallites in the large granules. Total crystallinity was systematically lower for the small granules, but their 9 nm SAXS peak was more intense. Small and large granular starch fractions of four European wheat varieties showed systematic but small differences in amylopectin chain length distribution. The more cooperative unwinding of double helices, prompted by DSC at 40% moisture, suggested longer double helices for the small wheat starch granules. The different evolutions of small-angle Bragg spacings on hydrating small and large granules furthermore indicated that the single-stranded parts connecting double helices to the amylopectin backbone are shorter in the small granules. The gelatinisation peak temperature (66% moisture) was higher for the small granule fractions. The large difference in small-angle scattering power and the higher gelatinisation temperatures probably results from a denser stacking of amylopectin double helices. The latter is governed by differences in amylopectin structure, and as only small differences in chain length distribution were found, differences are presumably due to variations in the location of α-(1–6) linkages. The progressive accumulation of crystallite defects during starch deposition may result in a larger average number of defects in large than in small wheat granules. In excess water, this triggers a collapse of the granular structure (gelatinisation) at lower temperatures for the large granules, which results in smaller gelatinisation ranges in view of its larger mass per granule.

Acknowledgements

RV acknowledges the ‘instituut voor de aanmoediging van Innovatie door Wetenschap en Technologie in

Vlaanderen' (IWT, Brussels, Belgium) for the receipt of a scholarship. BG is postdoctoral fellow of the 'Fonds voor Wetenschappelijk Onderzoek-Vlaanderen' (FWO-Flanders, Brussels, Belgium). BG, HR and JAD thank the FWO-Flanders for continuous support and equipment. Tate & Lyle Food Industrial Ingredients Europe (Aalst, Belgium) is thanked for the use of the Coulter Multisizer II. Helpful discussions with Prof. Maarten Geypens (Bodemkundige Dienst van België, Heverlee, Belgium) are acknowledged. Technical assistance by Dr Florean Meneau (DUBBLE CRG/ESRF, Grenoble, France), Dr Jan Vansteelandt and Luc Van den Ende (Laboratory of Food Chemistry, Katholieke Universiteit Leuven, Leuven, Belgium) is gratefully appreciated.

References

Ando, H., Tang, H. J., Watanabe, K., & Mitsunaga, T. (2002). Some physicochemical properties of large, medium and small granules starches in fractions of wheat grain. *Food Science and Technology Research*, *8*, 24–27.

Baruch, D. W., Meredith, P., Jenkins, L. D., & Simmons, L. D. (1979). Starch granules of developing wheat kernels. *Cereal Chemistry*, *56*, 554–558.

Blennow, A., Hansen, M., Schultz, A., Jørgensen, K., Donald, A. M., & Sanderson, J. (2003). The molecular deposition of transgenetically modified starch in the starch granule as imaged by functional microscopy. *Journal of Structural Biology*, *143*, 229–241.

Bocharnikova, I., Wasserman, L. A., Krivandin, A. V., Fornal, J., Blaszczak, W., Chernykh, V. Y., Schiraldi, A., & Yuryev, V. P. (2003). Structure and thermodynamic melting parameters of wheat starches with different amylose content. *Journal of Thermal Analysis and Calorimetry*, *74*, 681–695.

Buléon, A., Colonna, P., Planchot, V., & Ball, S. (1998). Starch granules: structure and biosynthesis. *International Journal of Biological Macromolecules*, *23*, 85–112.

Buléon, A, Colonna, P., Planchot, V., Gérard, C., Le Bail, P., Bizot, H. (1999). Genetic and environmental control of starch structure. Oral Presentation at the 50th Starch convention, Detmold.

Cameron, R. E., & Donald, A. M. (1992). A small-angle X-ray scattering study of the annealing and gelatinization of starch. *Polymer*, *33*, 2628–2636.

Chrastil, J. (1987). Improved colourimetric determination of amylose in starches or flours. *Carbohydrate Research*, *159*, 154–158.

Crist, B. (2000). Analysis of small-angle X-ray scattering patterns. *Journal of Macromolecular Science. Part B-Physics*, *39*, 493–518.

Dengate, H., & Meredith, P. (1984). Variation in size distribution of starch granules from wheat grain. *Journal of Cereal Science*, *2*, 83–90.

Donald, A. M. (2001). Plasticization and self assembly in the starch granule. *Cereal Chemistry*, *78*, 307–314.

Donald, A. M., Waigh, T. A., Jenkins, P. J., Gidley, M. J., Debet, M., Smith, A. (1997). Internal structure of starch granules revealed by scattering studies. In P. J. Frazier, A. M. Donald, & P. Richmond (Eds.), *Starch structure and functionality* (pp. 172–179). Cambridge: The Royal Society of Chemistry.

Donovan, J. W., & Mapes, C. J. (1980). Multiple phase transitions of starches and Naegeli amylodextrins. *Starch/Staerke*, *32*, 265–270.

Dubois, M., Gilles, K. A., Hamilton, J. K., Rebers, P. A., & Smith, F. (1956). Colorimetric method for determination of sugars and related substances. *Analytical Chemistry*, *28*, 350–356.

French, D. (1984). Organization of starch granules. In R. L. Whistler, J. N. BeMiller, & J. F. Paschall (Eds.), *Starch chemistry and technology* (pp. 183–247). San Diego, CA: Academic Press.

Gérard, C., Planchot, V., Colonna, P., & Bertoft, E. (2000). Relationship between branching density and crystalline structure of A- and B-type maize mutant starches. *Carbohydrate Research*, *326*, 130–144.

Goderis, B., Reynaers, H., Koch, M. H. J., & Mathot, V. B. F. (1999). Use of SAXS and linear correlation functions for the determination of the crystallinity and morphology of semi-crystalline polymers. Application to linear polyethylene. *Journal of Polymer Science. Part B-Polymer Physics*, *37*, 1715–1738.

Hanashiro, I., Tagawa, M., Shibahara, S., Iwata, K., & Takeda, Y. (2002). Examination of molar-based distribution of A, B and C chains of amylopectin by fluorescent labeling with 2-aminopyridine. *Carbohydrate Research*, *337*, 1211–1215.

Hizukuri, S. (1986). Polymodal distribution of the chain lengths of amylopectins, and its significance. *Carbohydrate Research*, *147*, 342–347.

Hizukuri, S. (1996). Starch: analytical aspects. In A. C. Eliasson (Ed.), *Carbohydrates in food* (pp. 347–429). New York: Marcel Dekker.

Hizukuri, S., Takeda, Y., Usami, S., & Takase, Y. (1980). Effect of aliphatic hydrocarbon groups on the crystallization of amylodextrin-model experiments for starch crystallization. *Carbohydrate Research*, *83*, 193–199.

Hoseney, R. C. (1994). *Principles of cereal science and technology*. St. Paul, MN: American Association of Cereal Chemists.

Huang, T. C., Toraya, H., Blanton, T. N., & Wu, Y. (1993). X-ray powder diffraction analysis of silver behenate, a possible low-angle diffraction standard. *Journal of Applied Crystallography*, *26*, 180–184.

Imberty, A., Buléon, A., Tran, V., & Pérez, S. (1991). Recent advances in knowledge of starch structure. *Starch/Staerke*, *43*, 375–384.

Jenkins, P. J., & Donald, A. M. (1995). The influence of amylose on starch granule structure. *International Journal of Biological Macromolecules*, *17*, 315–321.

Klucinec, J. D., & Thompson, D. B. (2002). Structure of amylopectins from ae-containing maize starches. *Cereal Chemistry*, *79*, 19–23.

Koch, K., Andersson, R., & Aman, P. (1998). Quantitative analysis of amylopectin unit chains by means of high-performance anion-exchange chromatography with pulsed amperometric detection. *Journal of Chromatography A*, *800*, 199–206.

Langeveld, S. M. J., van Wijk, R., Stuurman, N., Kijne, J. W., & de Pater, S. (2000). B-type granule containing protrusions and interconnections between amyloplasts in developing wheat endosperm revealed by transmission electron microscopy and GFP expression. *Journal of Experimental Botany*, *51*, 1357–1361.

MacGregor, A. W., & Morgan, J. E. (1986). Hydrolysis of barley starch granules by alpha-amylases from barley malt. *Cereal foods world*, *31*, 688–693.

Morrison, W. R., Milligan, T. P., & Azudin, M. N. (1984). A relationship between the amylose and lipid contents of starches from diploid cereals. *Journal of Cereal Science*, *2*, 257–271.

Myllärinen, P., Schulman, A. H., Salovaara, H., & Poutanen, K. (1998). The effect of growth temperature on gelatinization properties of barley starch. *Acta Agriculturae Scandinavica. Section B-Soil and Plant Science*, *48*, 85–90.

Oostergetel, G. Y., & van Bruggen, E. F. J. (1989). On the origin of the low angle spacing in starch. *Starch/Staerke*, *41*, 331–335.

O'Sullivan, A. C., & Pérez, S. (1999). The relationship between internal chain length of amylopectin and crystallinity in starch. *Biopolymers*, *50*, 381–390.

Peng, M., Gao, M., Abdel-Aal, E. S. M., Hucl, P., & Chibbar, R. N. (1999). Separation and characterization of A- and B-type starch granules in wheat endosperm. *Cereal Chemistry*, *76*, 375–379.

Peng, M., Gao, M., Båga, M., Hucl, P., & Chibbar, R. N. (2000). Starch-branching enzymes preferentially associated with A-type starch granules in wheat endosperm. *Plant Physiology*, *124*, 265–272.

Protserov, V. A., Karpov, V. G., Kozhevnikov, G. O., Wasserman, L. A., & Yuryev, V. P. (2000). Changes of thermodynamic and structural properties of potato starches (Udacha and Acrosil varieties) during biosynthesis. *Starch/Staerke*, *52*, 461–466.

Qi, X., Tester, R. F., Snape, C. E., Yuryev, V., Wasserman, L. A., & Ansell, R. (2004). Molecular basis of the gelatinisation and swelling characteristics of waxy barley starches grown in the same location during the same season, Part II. Crystallinity and gelatinisation characteristics. *Journal of Cereal Science*, *39*, 57–66.

Raeker, M. Ö., Gaines, C. S., Finney, P. L., & Donelson, T. (1998). Granule size distribution and chemical composition of starches from 12 soft wheat cultivars. *Cereal Chemistry*, *75*, 721–728.

Reddy, R. K., Ali, Z. S., & Bhattacharya, K. R. (1993). The fine structure of rice-starch amylopectin and its relation to the texture of cooked rice. *Carbohydrate Polymers*, *22*, 267–275.

Sahlström, S., Bævre, A. B., & Bråthen, E. (2003). Impact of starch properties on hearth bread characteristics II, Purified A- and B-granule fractions. *Journal of Cereal Science*, *37*, 285–293.

Shannon, J. C., & Garwood, D. L. (1984). Genetics and physiology of starch development. In R. L. Whistler, J. N. BeMiller, & J. F. Paschall (Eds.), *Starch chemistry and technology* (pp. 25–86). San Diego: Academic Press.

Shi, Y. C., Seib, P. A., & Bernardin, J. E. (1994). Effect of temperature during grain-filling on starches from six wheat cultivars. *Cereal Chemistry*, *71*, 369–383.

Somogyi, M. (1960). Modifications of two methods for the assay of amylase. *Clinical Chemistry*, *6*, 23–35.

Soulaka, A. B., & Morrison, W. R. (1985a). The amylose and lipid content, dimensions, and gelatinisation characteristics of some wheat starches and their A-granule and B-granule fraction. *Journal of the Science of Food and Agriculture*, *36*, 709–718.

Soulaka, A. B., & Morrison, W. R. (1985b). The bread baking quality of six wheat starches differing in composition and physical properties. *Journal of the Science of Food and Agriculture*, *36*, 719–727.

Stoddard, F. L., & Sarker, R. (2000). Characterization of starch in Aegilops species. *Cereal Chemistry*, *77*, 445–447.

Stribeck, N. (1993). SAXS data analysis of a lamellar two-phase system. *Layer statistics and compansion. Colloid and Polymer Science*, *271*, 1007–1023.

Tang, H., Ando, H., Watanabe, K., Takeda, Y., & Mitsunaga, T. (2001). Physicochemical properties of large, medium and small granule starches in fractions of normal barley endosperm. *Carbohydrate Research*, *330*, 241–248.

Vandeputte, G. E., Vermeylen, R., Geeroms, J., & Delcour, J. A. (2003). Rice starches I Structural aspects provide insight into crystallinity characteristics and gelatinisation behaviour of granular starch. *Journal of Cereal Science*, *38*, 43–52.

Vansteelandt, J., & Delcour, J. A. (1999). Characterisation of starch from durum wheat. *Starch/Staerke*, *73*, 73–80.

Vasanthan, T., & Bhatty, R. S. (1996). Physicochemical properties of small- and large-granule starches of waxy, regular, and high-amylose barleys. *Cereal Chemistry*, *73*, 199–207.

Vermeylen, R., Goderis, B., Reynaers, H., & Delcour, J. A. (2004). Amylopectin molecular structure reflected in macromolecular organization of granular starch. *Biomacromolecules*, *5*, 1775–1786.

Vonk, C. G. (1982). Synthetic polymers in the solid state. In O. Glatter, & O. Kratky (Eds.), *Small angle X-ray scattering* (pp. 433–466). London: Academic Press.

Waigh, T. A., Perry, P., Riekel, C., Gidley, M. J., & Donald, A. M. (1998). Chiral side-chain liquid-crystalline polymeric properties of starch. *Macromolecules*, *31*, 7980–7984.

Waigh, T. A., Gidley, M. J., Komanshek, B. U., & Donald, A. M. (2000). The phase transformations in starch during gelatinisation: a liquid crystalline approach. *Carbohydrate Research*, *328*, 165–176.

Wasserman, L. A., Eiges, N. S., Koltysheva, G. I., Andreev, N. R., Karpov, V. G., & Yuryev, V. P. (2001). The application of different physical approaches for the description of structural features in wheat and rye starches. A DSC study. *Starch/Staerke*, *53*, 629–634.

Whittam, M. A., Noel, T. R., & Ring, S. G. (1990). Melting behavior of A-type and B-type crystalline starch. *International Journal of Biological Macromolecules*, *12*, 359–362.

Yuryev, V. P., Krivandin, A. V., Kiseleva, V. I., Wasseman, L. A., Genkina, N. K., Fornal, J., Blaszczak, W., & Schiraldi, A. (2004). Structural parameters of amylopectin clusters and semi-crystalline growth rings in wheat starches with different amylose content. *Carbohydrate Research*, *339*, 2683–2691.